Spontaneous Pattern Formation in a Polariton Condensate

F. Manni,[1,*] K. G. Lagoudakis,[1] T. C. H. Liew,[2] R. André,[3] and B. Deveaud-Plédran[1]

[1]*Institute of Condensed Matter Physics, Ecole Polytechnique Fédérale de Lausanne (EPFL), CH-1015, Lausanne, Switzerland*
[2]*Institute of Theoretical Physics, Ecole Polytechnique Fédérale de Lausanne (EPFL), CH-1015 Lausanne, Switzerland*
[3]*Institut Néel, CNRS, Grenoble, France*

(Received 17 May 2011; published 2 September 2011)

Exciton-polariton condensation can be regarded as a self-organization phenomenon, where phase ordering is established among particles in the system. In such condensed systems, further ordering can occur in the particle density distribution, under particular experimental conditions. In this work we report on spontaneous pattern formation in a polariton condensate under nonresonant optical pumping. The slightly elliptical ring-shaped excitation laser that we employ forces condensation to occur into a single-energy state with periodic boundary conditions, giving rise to a multilobe standing-wave patterned state.

DOI: 10.1103/PhysRevLett.107.106401 PACS numbers: 71.35.Lk, 63.20.Pw, 67.10.Ba, 71.36.+c

Self-organization and pattern formation phenomena are among the most cross-sectional topics in science, as they range from the spontaneous folding of proteins in biology [1] and self-assembly of molecules [2] to liquid crystal ordering in chemistry [3,4]. The spontaneous symmetry breaking that accompanies polariton condensation [5–9] and superfluidity [10,11] can be interpreted as the manifestation of a self-organization process of particles in the system, where phase ordering is established at macroscopic scales. In such systems, under particular conditions, additional ordering may occur in the density distribution, giving rise to spatial patterns.

Polaritons, half-light half-matter quasiparticles, represent the eigenmodes of strongly interacting light and matter, which can be achieved in planar semiconductor microcavities endowed with quantum wells, in the strong coupling regime [12]. Spatial localization of polaritons can be achieved on the micrometer scale due to their small effective mass [7], coming from their photonic component. A successful approach, in order to study the polariton phenomenology in lower dimensionality, consists in the localization of polaritons via the confinement of the photonic component through nanostructuring of the planar two-dimensional microcavity, leading to both 1D and 0D polariton states, as in [8,13,14]. In these works the confinement of the polariton wave function comes from the real potential created by the structure realized in the samples. Other studies have rather focused on polariton localization effects and spatial inhomogeneous condensation due to the presence of photonic disorder, a feature naturally arising in semiconductor microcavities as a result of the growth processes of the samples. Disorder and multimode condensation in spatially overlapping modes has been extensively studied [15], while a laserlike gain-induced mechanism for polariton localization because of the excitation spot has also been reported [16] in a disordered potential.

In this Letter we demonstrate an all-optical spontaneous patterning of the density of a polariton condensate within the ring geometry of the nonresonant excitation laser. The laser acts, through a gain-loss mechanism, in favor of localization of polaritons in a ringlike geometry with a condensate wave function (order parameter) satisfying periodic boundary conditions. The cylindrical symmetry of the system is broken by the small ellipticity of the excitation intensity profile. This causes polaritons to condense in an elliptical multilobe patterned single-energy state, with analogous features to the ones seen in polariton microwires [8]. We nonresonantly create the polariton condensate and, thus, we do not imprint any phase distribution directly with the pump laser. The observed phenomenology and the pattern formation mechanism are reproduced through a theoretical model based on the generalized Gross-Pitaevskii equation [17].

Our experimental setup is depicted in Fig. 1(a). The sample, the same CdTe semiconductor microcavity of [7], is kept in a cold-finger cryostat at liquid helium temperature (≈ 4 K). The nonresonant optical excitation is provided by a quasicontinuous-wave Ti:sapphire monomode laser. We employ an optical lossless technique which involves the use of an axicon, a conical lens that is able to convert an input Gaussian beam into an output laser beam with a ring intensity distribution. We are able to finely tune the size and ensure the homogeneity of the laser ring by finely adjusting the axicon position with respect to the subsequent focusing lenses using x-y-z micrometric translation stages. The properly shaped laser beam is then focused on the surface of the sample through a high numerical aperture (0.5 NA) microscope objective. The same objective collects the luminescence emitted by the sample that is sent towards a modified Mach-Zehnder interferometer, which allows us to measure both condensate density and phase. Since we are using nonresonant excitation, a traditional homodyne detection scheme is not applicable to our case. Therefore, we implemented a customized version of the Mach-Zehnder interferometer in which one of the two arms, the so-called reference arm

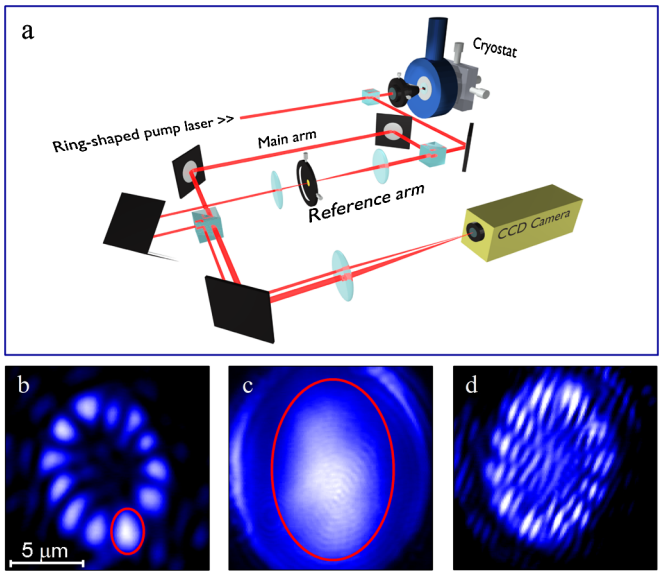

FIG. 1 (color online). (a) Experimental setup. The ring-shaped laser, obtained using an axicon lens, is focused on the sample through a 0.5 NA microscope objective. The same objective collects the PL signal, which is then sent to a modified Mach-Zehnder interferometer. The luminescence coming from the sample, shown in (b), is overlapped with a selected region of itself [marked by the red ellipse in (b) and (c)] to obtain the resulting interferogram (d). Note that the real-space density in (b) is acquired here for a pump power of 300 μW, showing that the pattern remains identical for pump powers higher than the condensation threshold.

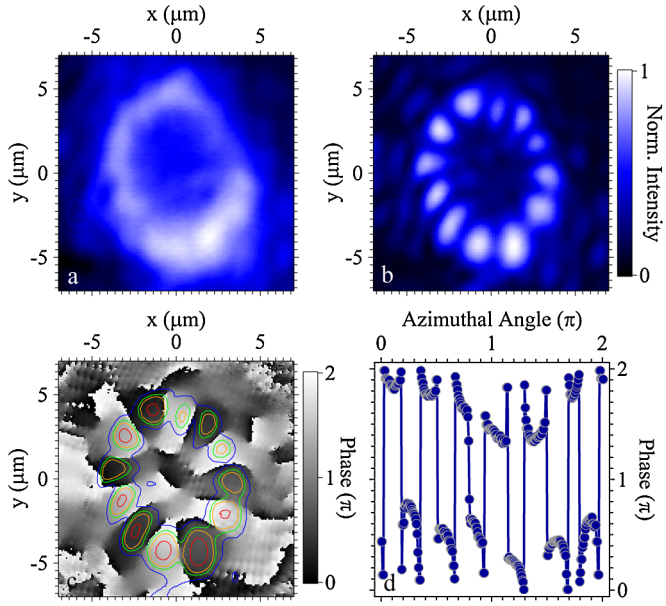

FIG. 2 (color online). (a) Polariton density below condensation threshold under ring-shaped laser excitation. (b) Polariton density above condensation threshold. The spontaneous formation of a spatial pattern, made up of 12 lobes, can be clearly observed. (c) Phase map corresponding to the polariton density shown in (b) where a density contour plot is superimposed in order to allow identification of the density lobes in the phase structure. (d) Phase profile along the patterned density ring, where the phase jumps between successive lobes can be identified.

[Fig. 1(c)], is a magnified version of the other one, which we call the main arm [Fig. 1(b)] or photoluminescence (PL) arm [see sketch of Fig. 1(a)]. The magnification of the reference is set to 4 times with respect to the main arm by the choice of the focal lengths of the two-lens telescope. A pinhole allows us to filter in real space the portion of the magnified PL [giving rise to some residual Airy fringes visible in the outer margins in Fig. 1(c)] that we want to overlap with the main arm to get an interference pattern, an example of which is shown in Fig. 1(d). Fine-tuning of the output optical cube allows us to select at will the overlap conditions between the two arms, while lateral and vertical shifts of the retroreflector result in a controlled wave vector mismatch between the two interfering beams, making it possible to set the density and the direction of the interference fringes.

For a pump power of 100 μW we are below the polariton condensation threshold and the resulting detected photoluminescence signal is the one shown in Fig. 2(a). The PL signal, as the excitation laser, is in turn ring shaped. Despite the homogeneity of the prepared laser ring (not shown), it can be seen that the PL is slightly affected by the natural disordered potential present at this specific position in the sample. This results in a higher intensity at one of the two sides of the PL ring. As condensation threshold is reached [as shown in Fig. 2(b)], for a pump power of around 250 μW, we observe the sudden spontaneous appearance of a single-energy condensed state of polaritons featuring a clear pattern of 12 lobes along the ring. Another feature worth noting in Fig. 2(b) is that the polariton density in the lobes is still affected by the presence of the natural disorder: the local blueshift along the ring is such to lock the phase between the various lobes and form a single-energy state in agreement with the mode-synchronization mechanism [18] also observed in the case of one-dimensional polariton condensates in a disordered potential [19].

A tomographic reconstruction of the real-space emission at the energy of the condensate (see Supplemental Material [20]) shows that, for pump powers just above threshold, polariton condensation indeed occurs in a single-energy state. The energy resolved pattern matches perfectly well the spectrally integrated PL. Further increasing the excitation power we keep observing the same spatial pattern, up to almost 2 times the condensation threshold. For even higher excitation powers, condensation starts to take place in multiple spatially overlapping modes [15]. Condensation in a single-energy mode allows us to directly extract the phase even from an energy-integrated interferogram, since the corresponding phase distribution only comes from the condensed state.

The phase extraction from the interferogram image is based on digital holography techniques, as in our previous

works [21,22]. In the modified Mach-Zehnder interferometer, the reference arm is chosen to be one of the lobes of the density pattern, providing an approximately flat reference phase for the whole interferogram. The interference pattern we obtain is shown in Fig. 2(c). In the phase distribution, the 12-lobe density structure can be easily identified, each lobe having a well-defined phase. Between each lobe and its two nearest neighbors it is expected from theory (see below) to have a phase jump of the order of π, in agreement with the phase profile extracted along the patterned ring [see Fig. 2(d)].

Polariton condensates generated with a nonresonant pump represent a highly nonequilibrium system. While the polariton condensate itself can be accurately described by a mean-field approximation, it is essential in a full theoretical treatment to also account for the incoherent excitations generated by nonresonant pumping that couple to the condensate. An intuitive description makes use of a Gross-Pitaevskii-type equation for the condensate mean field, coupled to a classical rate equation for the dynamics of an exciton reservoir [17]. Such a description has been used to model both spectral and spatial features [16,23] and adapted to dynamic properties [24–26] of polariton condensates. It reads:

$$i\hbar\frac{\partial\psi(\mathbf{r},t)}{\partial t} = \left\{\hat{E}_{LP} + V(\mathbf{r}) + \frac{i\hbar}{2}[R_R n(\mathbf{r},t) - \gamma_c]\right\}\psi(\mathbf{r},t), \tag{1}$$

$$\frac{\partial n(\mathbf{r},t)}{\partial t} = -(\gamma_R + R_R|\psi(\mathbf{r},t)|^2)n(\mathbf{r},t) + P(\mathbf{r}), \tag{2}$$

where $\psi(\mathbf{r},t)$ is the mean field representing the polariton condensate and $n(\mathbf{r},t)$ is the intensity distribution of an incoherent excitonic reservoir. For simplicity we neglect the polarization degree of freedom. $\hat{E}_{LP}$ is the polariton kinetic energy operator, which represents the nonparabolic dispersion of lower branch polaritons. $V(\mathbf{r})$ represents an induced effective potential, given by the mean-field shift caused by polariton-polariton interactions (g), the interaction of polaritons with the reservoir (g_R) and an additional pump induced shift (G) [17]; $V(\mathbf{r}) = \hbar g|\psi(\mathbf{r},t)|^2 + \hbar g_R n(\mathbf{r},t) + \hbar G P(\mathbf{r})$, where g, g_R, and G are constants. $P(\mathbf{r})$ represents the spatial pump distribution (see Supplemental Material [20]). Although interactions between polaritons inside the condensate are present, the dominant effective potential terms are arising from the effect of the exciton reservoir on condensed polaritons [16]. γ_c and γ_R represent the decay rates of condensed polaritons and reservoir excitons, respectively. R_R is the condensation rate. Equations (1) and (2) can be solved numerically in time until a steady state is reached starting from an initial random phase (white noise) and low intensity distribution for $\psi(\mathbf{r},0)$. Using a slightly elliptical ring-shaped pump and solving the equations for the steady state indeed leads to ring-shaped multilobed spontaneous polariton patterns for parameters corresponding to our experiment [27]. Figure 3 shows the resulting polariton intensity and phase calculated with this method. Within our theory, the number of lobes is quite sensitive to the profile of the pump. For slightly larger sized rings we have computed up to 24 lobes. Experimentally, we also find that the number of lobes is sensitive to the ring diameter and to the position on the sample, because of disorder (which we do not include in the theoretical model for simplicity). Disorder enters in the determination of the energy of the condensate, as it influences the potential landscape, as well as in the kinetic energy term for the particles, since it determines their flows. Therefore disorder is affecting the state at which condensation takes place and the corresponding standing-wave pattern can have a different number of lobes. Overall, the pattern formation effect itself is robust enough to withstand disorder perturbations and is quite generic on the sample surface. Theoretically a π phase flip is observed between neighboring lobes, in agreement with the experimentally measured phase distribution, shown in Fig. 2(c).

Qualitatively, the pattern formation can be interpreted as a consequence of condensation into a single-energy state with periodic boundary conditions. The optically induced localization generates a spectrally discrete set of "standing-wave" modes, which differ in the number of angular nodes. In a perfectly cylindrically symmetric system, each energy level would be twofold degenerate, since eigenstates composed from symmetric and antisymmetric linear combinations of states with equal and opposite orbital angular momentum are both possible. Without any mechanism to break this symmetry, one would expect a cylindrically symmetric density distribution to be excited and no pattern formation to occur. However, in the geometry we are dealing with here, the symmetry is not perfectly cylindrical due to the slight elliptical shape of the pump laser beam. In this case the degeneracy between symmetric and antisymmetric states is lifted and polariton condensation takes place into a state featuring a multilobe spatial pattern. The single-energy condensed state, as reproduced

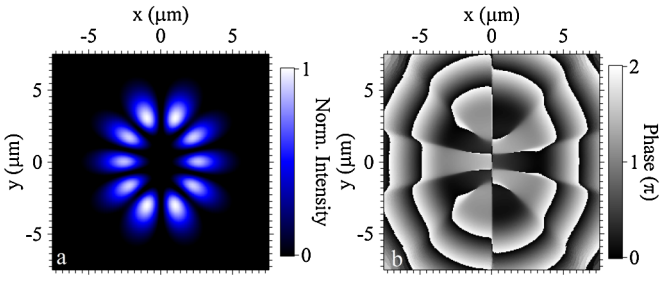

FIG. 3 (color online). Results of the simulations performed with a generalized Gross-Pitaevskii-based model under nonresonant (slightly elliptical) ring-shaped laser excitation. (a) Polariton density of a 10-lobe spatial pattern and (b) phase distribution.

in the theoretical simulations, results from a complex interplay between the localization effect of the narrow excitation ring profile and the nonequilibrium pump-decay processes for the polariton system.

The situation can be considered, to some extent, analogous to the case of condensation in a polariton microwire [8,23] where the states are nondegenerate one-dimensional standing waves. When polariton condensation occurs into one of those modes it is clear that a pattern in intensity appears, given by the standing-wave profile. In our case, instead of using a real potential, we are able to achieve a spontaneous pattern formation in a ring-shaped system with periodic boundary conditions using all-optical means, as we are able to provide with the same excitation beam both the pumping and the localization.

In this work we have reported on the spontaneous pattern formation of an all optically induced quasi-one-dimensional polariton condensate with periodic boundary conditions, under nonresonant optical excitation. The slightly elliptical ring-shaped intensity profile of the laser, that is used to pump the system, is also responsible for the symmetry breaking. In these conditions polariton condensation is found to occur in a single-energy state, featuring a multilobe density pattern. The theoretical description we provide, based on a mean-field Gross-Pitaevskii equation, is able to reproduce the experimental findings, capturing the physics of the observed spontaneous pattern formation phenomenology in a polariton condensate.

We would like to thank Y. Leger, M. Wouters, and V. Savona for fruitful discussions. This work was supported by the Swiss National Science Foundation through NCCR ''Quantum Photonics.''

*francesco.manni@epfl.ch

[1] E. Karsenti, Nat. Rev. Mol. Cell Biol. **9**, 255 (2008).
[2] G. M. Whitesides, J. P. Mathias, and C. T. Seto, Science **254**, 1312 (1991).
[3] J. M. Lehn, Science **295**, 2400 (2002).
[4] G. Ungar, Y. S. Liu, X. B. Zeng, V. Percec, and W. D. Cho, Science **299**, 1208 (2003).
[5] R. Balili, V. Hartwell, D. Snoke, L. Pfeiffer, and K. West, Science **316**, 1007 (2007).
[6] H. Deng, G. S. Solomon, R. Hey, K. H. Ploog, and Y. Yamamoto, Phys. Rev. Lett. **99**, 126403 (2007).
[7] J. Kasprzak *et al.*, Nature (London) **443**, 409 (2006).
[8] E. Wertz *et al.*, Nature Phys. **6**, 860 (2010).
[9] C. W. Lai *et al.*, Nature (London) **450**, 529 (2007).
[10] A. Amo, J. Lefrère, S. Pigeon, C. Adrados, C. Ciuti, I. Carusotto, R. Houdre, E. Giacobino, and A. Bramati, Nature Phys. **5**, 805 (2009).
[11] A. Amo *et al.*, Nature (London) **457**, 291 (2009).
[12] C. Weisbuch, M. Nishioka, A. Ishikawa, and Y. Arakawa, Phys. Rev. Lett. **69**, 3314 (1992).
[13] R. I. Kaitouni *et al.*, Phys. Rev. B **74**, 155311 (2006).
[14] R. Cerna *et al.*, Phys. Rev. B **80**, 121309 (2009).
[15] D. N. Krizhanovskii *et al.*, Phys. Rev. B **80**, 045317 (2009).
[16] G. Roumpos, W. H. Nitsche, S. Hofling, A. Forchel, and Y. Yamamoto, Phys. Rev. Lett. **104**, 126403 (2010).
[17] M. Wouters, I. Carusotto, and C. Ciuti, Phys. Rev. B **77**, 115340 (2008).
[18] A. Baas, K. G. Lagoudakis, M. Richard, R. André, L. S. Dang, and B. Deveaud-Plédran, Phys. Rev. Lett. **100**, 170401 (2008).
[19] F. Manni, K. G. Lagoudakis, B. Pietka, L. Fontanesi, M. Wouters, V. Savona, R. André, and B. Deveaud-Plédran, Phys. Rev. Lett. **106**, 176401 (2011).
[20] See Supplemental Material at http://link.aps.org/supplemental/10.1103/PhysRevLett.107.106401 for the energy-resolved tomographic reconstruction of the condensate density and a detailed description of the parameters used in the simulations.
[21] K. G. Lagoudakis, M. Wouters, M. Richard, A. Baas, I. Carusotto, R. André, L. S. Dang, and B. Deveaud-Plédran, Nature Phys. **4**, 706 (2008).
[22] K. G. Lagoudakis, T. Ostatnicky, A. V. Kavokin, Y. G. Rubo, R. André, and B. Deveaud-Plédran, Science **326**, 974 (2009).
[23] M. Wouters, T. C. H. Liew, and V. Savona, Phys. Rev. B **82**, 245315 (2010).
[24] G. Nardin, K. G. Lagoudakis, M. Wouters, M. Richard, A. Baas, R. André, L. S. Dang, B. Pietka, and B. Deveaud-Plédran, Phys. Rev. Lett. **103**, 256402 (2009).
[25] K. G. Lagoudakis, B. Pietka, M. Wouters, R. André, and B. Deveaud-Plédran, Phys. Rev. Lett. **105**, 120403 (2010).
[26] K. G. Lagoudakis, F. Manni, B. Pietka, M. Wouters, T. C. H. Liew, V. Savona, A. V. Kavokin, R. André, and B. Deveaud-Plédran, Phys. Rev. Lett. **106**, 115301 (2011).
[27] We used the following parameters in the simulations: $\hbar\gamma_c = 1$ meV, $\hbar\gamma_R = 10$ meV, $\hbar R_R = 0.1$ meV μm^2, $G = 0.005$ μm^2, $\hbar g_R = 0.022$ meV μm^2. The polariton dispersion was calculated with the standard two oscillator model with effective cavity photon mass 3×10^{-5} of the free electron mass and 26 meV Rabi splitting. The pump had an ellipticity of approximately 0.9 (see Supplemental Material [20]).